



# Identifying soil N<sub>2</sub>O sources by combining laboratory experiments with process-based models

Zhifeng Yan<sup>1</sup> · Zhaopei Chu · Balázs Grosz · Baoxuan Chang ·  
Narasinha Shurpali · Gang Liu · Zhaolei Li · Jinsen Zheng · Si-liang Li ·  
Klaus Butterbach-Bahl

Received: 10 February 2025 / Accepted: 22 May 2025 / Published online: 9 October 2025  
© The Author(s) 2025

**Abstract** Nitrification and denitrification are two important biological processes producing N<sub>2</sub>O in soils, but their contributions to N<sub>2</sub>O emissions are not well understood, hindering precise mitigation measures. Here, we developed process-based models (PBM) with and without transport (T) to partition N<sub>2</sub>O sources by tracking nitrogen flows (NF) through

different reaction pathways. The model with transport (PBM-T-NF) well predicted N<sub>2</sub>O production from nitrification and denitrification in two different repacked soils with a shallow depth of 8 mm under moisture conditions ranging from 40 to 100% water-filled pore space (WFPS), demonstrating its robustness and reliability. In comparison, the model without transport (PBM-NF) failed to capture the N<sub>2</sub>O dynamics and the relative contribution of denitrification to N<sub>2</sub>O production ( $C_D$ ), highlighting the need of including mass transport in predicting N<sub>2</sub>O dynamics. The PBM-T-NF model was further employed to

Responsible Editor: Naomi Wells.

**Supplementary Information** The online version contains supplementary material available at <https://doi.org/10.1007/s10533-025-01246-3>.

Z. Yan (✉) · Z. Chu · B. Chang · S. Li  
Institute of Surface-Earth System Science, School of Earth System Science, Tianjin University, Tianjin 300072, China  
e-mail: yanzf17@tju.edu.cn

Z. Yan · S. Li  
Critical Zone Observatory of Bohai Coastal Region,  
Tianjin Key Laboratory of Earth Critical Zone Science  
and Sustainable Development in Bohai Rim, Tianjin  
University, Tianjin 300072, China

B. Grosz  
Thünen Institute of Climate-Smart Agriculture,  
38116 Brunswick, Germany

N. Shurpali  
Natural Resources Institute Finland, Halolantie 31 A,  
71750 Maaninka, Finland

G. Liu  
College of Management and Economics, Tianjin  
University, Tianjin 300072, China

Z. Li  
Key Laboratory of Low-Carbon Green Agriculture  
in Southwestern China, Ministry of Agriculture and Rural  
Affairs, Interdisciplinary Research Center for Agriculture  
Green Development in Yangtze River Basin, College  
of Resources and Environment, Southwest University,  
Chongqing, China

J. Zheng  
Crop, Livestock and Environment Division, Japan  
International Research Center for Agricultural Sciences,  
Ohwashi 1-1, Tsukuba, Ibaraki 305-8686, Japan

K. Butterbach-Bahl  
Institute of Meteorology and Climate Research,  
Atmospheric Environmental Research, Karlsruhe Institute  
of Technology, Garmisch-Partenkirchen, Germany

K. Butterbach-Bahl  
Pioneer Center Land-CRAFT, Agroecology, Aarhus  
University, Aarhus C, Denmark

investigate the effects of soil properties on  $N_2O$  emissions and sources. Increased  $NH_4^+$  concentration significantly decreased  $C_D$  under relatively low moisture conditions, while increased  $NO_3^-$  slightly promoted  $C_D$  over different moisture contents, emphasizing the importance of substrate availability and moisture conditions in controlling  $C_D$ . Furthermore, the PBM-T-NF model was used to quantify  $N_2O$  sources from an artificial soil core of 80 mm depth. Soil depth was shown to be important in mediating  $C_D$  by controlling  $O_2$  diffusivity, which is highly dependent on moisture content. Given the long-standing challenge in experimental quantification of  $N_2O$  sources from soils, our developed model provides a novel way to estimate  $N_2O$  production from different nitrogen processes, which is key for accurately targeting mitigation of  $N_2O$  emissions from soils.

**Keywords** Nitrification · Denitrification · Nitrous oxide · Process-based model · Mass transport

## Introduction

Nitrous oxide ( $N_2O$ ) plays an important role in driving global warming and depleting stratospheric ozone (IPCC 2021). Natural and managed soils are major sources of atmospheric  $N_2O$ , accounting for about half ( $7.9 \text{ Tg yr}^{-1}$ ) of emissions from 2007 to 2016 (Tian et al. 2020). However, this estimate of  $N_2O$  emissions is highly uncertain, ranging from 6.3–10.3  $\text{Tg yr}^{-1}$  (Tian et al. 2020), largely because the complicated processes that produce, transport and consume  $N_2O$  are difficult to be accurately characterized and incorporated in models that estimate global  $N_2O$  emissions (Butterbach-Bahl et al. 2013; Müller et al. 2014).

Nitrification and denitrification are the two primary biological processes that produce  $N_2O$  in soils (Wang et al. 2023). The magnitude of  $N_2O$  emission and its attribution from nitrification and denitrification are influenced by various environmental factors, such as substrate availability (Laville et al. 2011),  $O_2$  concentration (Song et al. 2019), and soil structure and texture (Lucas et al. 2023). Soil moisture is a key regulator of  $N_2O$  emissions and sources, mainly by modulating substrate and  $O_2$  availability (Smith 2017). As soil moisture increases, the rate of  $N_2O$  production is expected to decrease after reaching a maximum value, and the moisture tipping point

(i.e., the optimal water content) at which the maximum  $N_2O$  flux rate occurs varies with soil properties (Davidson et al. 2000). In general, nitrification dominates soil  $N_2O$  emissions under relatively low moisture conditions, while denitrification dominates under high moisture conditions (Han et al. 2024; Kool et al. 2011, 2007). Therefore, quantification of  $N_2O$  production from the two processes under different moisture conditions is critical for accurate estimation of soil  $N_2O$  emissions.

Several approaches have been employed to quantify soil  $N_2O$  production from nitrification and denitrification (Bateman and Baggs 2005; Groffman et al. 2006; Heinen 2006). Inhibitors, such as acetylene ( $C_2H_2$ ), have been widely used to separate nitrification and denitrification due to their simplicity and low cost (Bateman and Baggs 2005; Watts and Seitzinger 2000). However, this approach has been reported to systematically underestimate  $N_2O$  production from denitrification (Watts and Seitzinger 2000). In comparison, isotopic techniques, including natural and enrichment abundance approaches, have been shown to be more reliable in distinguishing different nitrogen (N) processes (Kool et al. 2011; Wang et al. 2024; Yang et al. 2019; Zhu et al. 2013). In particular, enrichment approaches with  $^{15}N-NH_4^+$  and/or  $^{15}N-NO_3^-$  additions have been widely used especially in agricultural soils (Bateman and Baggs 2005; Wang et al. 2023; Zhang et al. 2015), providing valuable insights into  $N_2O$  sources and the underlying mechanisms (Friedl et al. 2021; Wang et al. 2024). Furthermore, the natural isotope techniques, such as  $^{15}N$  site preference, can quantify  $N_2O$  emissions from different N processes without interfering with soil N cycling (Butterbach-Bahl et al. 2013), and are mostly applied in the field (Wei et al. 2023). Although N isotope data have been applied to constrain soil  $N_2O$  emissions at global scale (Harris et al. 2022), conclusions derived from  $^{15}N$  signals are often site- or soil-specific, and the high cost of isotopic techniques also limits their applications on a large scale (Ruser et al. 2006; Wei et al. 2023). The use of models provides another effective means of deriving regional or global  $N_2O$  estimates and to target mitigation options.

A large number of models have been developed to simulate  $N_2O$  emissions from soils (Butterbach-Bahl et al. 2013; Heinen 2006; Tian et al. 2018). Emission factor approaches are often used at regional or global scales, when the data needed to calculate  $N_2O$

emissions across spatial and temporal scales are not available (Wang et al. 2020a). These approaches are straightforward, but also have large uncertainties (Del Grosso et al. 2020). In comparison, process-based models are typically more accurate when applied at the site or farm scale (Ehrhardt et al. 2018; Yue et al. 2019). Numerous process-based models have been proposed to simulate N<sub>2</sub>O emissions with varying complexities (Del Grosso et al. 2020; Tian et al. 2019). The simplified ones, such as DAISY, often correlate N<sub>2</sub>O flux with estimates of soil N cycling (Hansen 2002); the detailed ones, such as SLIM, further account for the effects of soil structure on gas diffusion (Vinten et al. 1996); and the advanced ones, such as DNDC, explicitly quantify the dynamics of different microbial functional groups (Li et al. 2000). Most process-based models include N<sub>2</sub>O production from nitrification and denitrification (Butterbach-Bahl et al. 2013; Tian et al. 2019), where empirical relationships between N<sub>2</sub>O flux and environmental factors are widely applied (Del Grosso et al. 2000; Wang et al. 2021). In particular, the response of N<sub>2</sub>O fluxes to changes in soil moisture, i.e., moisture reduction functions, are highly soil specific (Friedl et al. 2021), and their empirical application in process-based models is a major source of uncertainty in N<sub>2</sub>O estimate (Heinen 2006). Furthermore, although <sup>15</sup>N signals have been employed in models to distinguish various N processes and quantify N<sub>2</sub>O emissions, these models, including a variety of N trace models (Jansen-Willems et al. 2022; Müller et al. 2014; Zheng et al. 2023), often use optimization technique such as Markov Chain Monte Carlo (MCMC) to quantify different N processes. By contrast, the combination of process-based models and N isotopic approaches are less explored.

Soil N<sub>2</sub>O emission is an integral consequence of N<sub>2</sub>O production, transport, and consumption (Butterbach-Bahl et al. 2013; Müller et al. 2014). As water is relatively stagnant in soils, the transport of N<sub>2</sub>O inside soils is mainly determined by gas diffusivity (Yan et al. 2018b), since gas diffuses in air approximately ten thousand faster than in water (Stumm and Morgan 1996). Moreover, the gas diffusivity is highly dependent on soil structure and moisture contents (Fu et al. 2024; Yan et al. 2016), whose interactions make soil N<sub>2</sub>O emissions difficult to predict (Rabot et al. 2015). Current models, including DLEM, APSIM and DayCent, often neglect the transport of

N<sub>2</sub>O in soils by assuming that the produced N<sub>2</sub>O is directly released to atmosphere, partly because the soil gas diffusivity is difficult to quantify experimentally (Tian et al. 2018; Parton et al. 1996; Del Grosso et al. 2020). This assumption is generally valid under low moisture condition but likely overestimates N<sub>2</sub>O emissions under high moisture conditions, in which part of N<sub>2</sub>O is reduced to N<sub>2</sub> due to their long retention time (Baggs 2011). Only a few models directly quantify the gas diffusion in soil profile (Li et al. 2000; Klier et al. 2011). For example, the DNDC model quantifies O<sub>2</sub> diffusion to determine the redox potential in soils, but neglects N<sub>2</sub>O diffusion along soil profiles (Li et al. 2000). Therefore, it is necessary to incorporate N<sub>2</sub>O transport in model simulations.

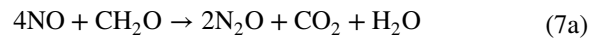
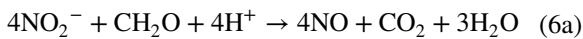
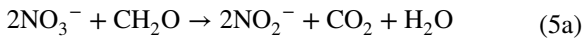
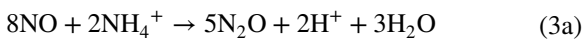
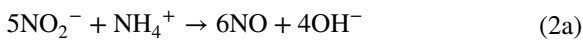
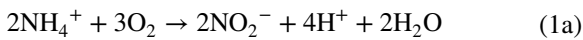
To better simulate soil N<sub>2</sub>O emissions and sources, here we: (1) developed process-based models (PBM) with and without transport (T) to quantify N<sub>2</sub>O production from nitrification and denitrification by tracking nitrogen flows (NF) in their reaction pathways; (2) evaluated the developed models by using incubation experiments, in which enriched <sup>15</sup>N techniques were applied to measure N<sub>2</sub>O emissions from nitrification and denitrification under six moisture levels (40–100% WFPS) (Wang et al. 2023); and (3) used the model with transport (PBM-T-NF) to investigate the effects of soil conditions on N<sub>2</sub>O emissions and sources. The PBM-T-NF model explicitly quantified the transport of solutes (i.e., dissolved N species, dissolved organic carbon, and dissolved O<sub>2</sub>) and gases (i.e., NO, N<sub>2</sub>O, N<sub>2</sub>, and O<sub>2</sub>) inside soils as well as their impacts on N<sub>2</sub>O production and consumption, which together determine N<sub>2</sub>O emissions. To focus on diffusion process, other transport processes such as advection were not included in the models, and the diffusion was described by Fick's Law (Yan et al. 2018a). By tracking the N flows through nitrification and denitrification based on <sup>15</sup>N signals, the developed models are also able to reliably quantify the contribution of nitrification and denitrification to N<sub>2</sub>O emissions under different environmental conditions. Consequently, the developed model is able to evaluate the effects of solutes and gases diffusion on N<sub>2</sub>O emissions, and quantify their attributions from nitrification and denitrification, which may reduce the uncertainty of estimating N<sub>2</sub>O emissions from soils.

## Methods

### Partition of N<sub>2</sub>O sources by tracking nitrogen flows

To simplify the model development and avoid over-parameterization, the developed models only accounted for the two most important pathways producing N<sub>2</sub>O (i.e., nitrification and denitrification) and neglected other microbial processes such as anaerobic ammonium oxidation (ANAMMOX) and chemical processes such as chemodenitrification. The reaction pathways used in the models are depicted in Fig. 1a.

Accordingly, the stoichiometry of each reaction pathway is described as follows, where Eqs. (1a–4a) represent nitrification and Eqs. (5a–8a) represent denitrification (Maggi et al. 2008):



Microbes (i.e., nitrifier and denitrifier communities) were explicitly considered in the models. Dual Michaelis–Menten kinetic equations were used to calculate the reaction rate ( $r$ ) for each pathway, and the  $r$  of denitrification was inhibited by O<sub>2</sub> concentration (Chang et al. 2022).

$$r_{\text{NH}_4^+ \rightarrow \text{NO}_2^-, \text{N}} = -\mu_{\text{NH}_4^+ \rightarrow \text{NO}_2^-} \cdot X_{\text{AOB}} \cdot \frac{C_{\text{NH}_4^+}}{C_{\text{NH}_4^+} + K_{\text{NH}_4^+, \text{NH}_4^+ \rightarrow \text{NO}_2^-}} \cdot \frac{C_{\text{O}_2, \text{a}}}{C_{\text{O}_2, \text{a}} + K_{\text{O}_2, \text{NH}_4^+ \rightarrow \text{NO}_2^-}} \quad (1b)$$

$$r_{\text{NO}_2^- \rightarrow \text{NO}, \text{N}} = -\mu_{\text{NO}_2^- \rightarrow \text{NO}, \text{N}} \cdot X_{\text{AOB}} \cdot \frac{C_{\text{NO}_2^-}}{C_{\text{NO}_2^-} + K_{\text{NO}_2^-, \text{NO}_2^- \rightarrow \text{NO}, \text{N}}} \cdot \frac{C_{\text{NH}_4^+}}{C_{\text{NH}_4^+} + K_{\text{NH}_4^+, \text{NO}_2^- \rightarrow \text{NO}}} \quad (2b)$$

$$r_{\text{NO} \rightarrow \text{N}_2\text{O}, \text{N}} = -\mu_{\text{NO} \rightarrow \text{N}_2\text{O}, \text{N}} \cdot X_{\text{AOB}} \cdot \frac{C_{\text{NO}, \text{a}}}{C_{\text{NO}, \text{a}} + K_{\text{NO}, \text{NO} \rightarrow \text{N}_2\text{O}, \text{N}}} \cdot \frac{C_{\text{NH}_4^+}}{C_{\text{NH}_4^+} + K_{\text{NH}_4^+, \text{NO} \rightarrow \text{N}_2\text{O}}} \quad (3b)$$

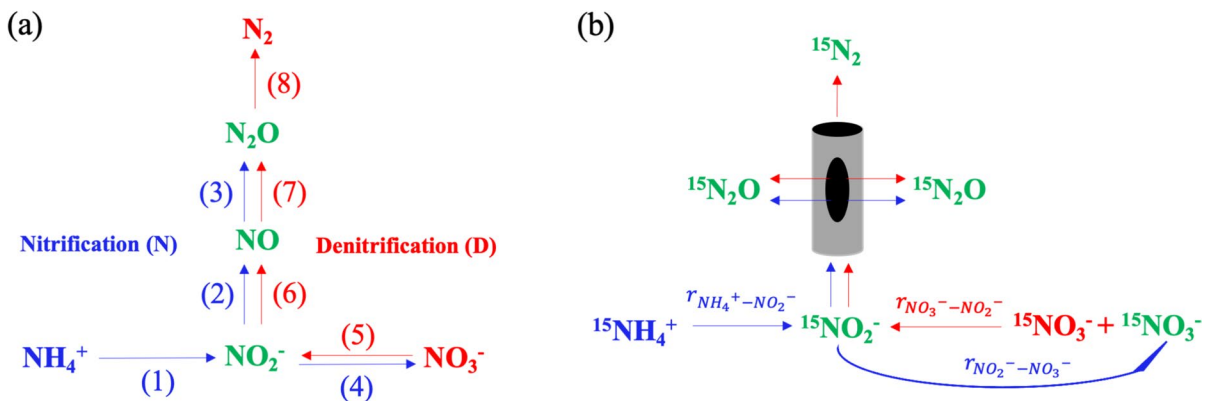


**Fig. 1** **a** Reaction pathways of nitrification and denitrification considered in this study. **b** Illustration showing the N flows of producing N<sub>2</sub>O as indicated by <sup>15</sup>N. The numbers in **a** refer to

the corresponding reaction pathways in the text, and the reactions ( $r$ ) in **b** can be found in the text

$$r_{NO_2^- \rightarrow NO_3^-, N} = -\mu_{NO_2^- \rightarrow NO_3^-, N} \cdot X_{NOB} \cdot \frac{C_{NO_2^-}}{C_{NO_2^-} + K_{NO_2^-, NO_2^- \rightarrow NO_3^-}} \cdot \frac{C_{O_{2,a}}}{C_{O_{2,a}} + K_{O_2, NO_2^- \rightarrow NO_3^-}} \quad (4b)$$

$$r_{NO_3^- \rightarrow NO_2^-, D} = -\mu_{NO_3^- \rightarrow NO_2^-, D} \cdot X_{DEN} \cdot \frac{C_{NO_3^-}}{C_{NO_3^-} + K_{NO_3^-, NO_3^- \rightarrow NO_2^-}} \cdot \frac{C_{DOC}}{C_{DOC} + K_{DOC, NO_3^- \rightarrow NO_2^-}} \cdot \frac{I_{O_2, NO_3^- \rightarrow NO_2^-, D}}{C_{O_{2,a}} + I_{O_2, NO_3^- \rightarrow NO_2^-, D}} \quad (5b)$$

$$r_{NO_2^- \rightarrow NO, D} = -\mu_{NO_2^- \rightarrow NO, D} \cdot X_{DEN} \cdot \frac{C_{NO_2^-}}{C_{NO_2^-} + K_{NO_2^-, NO_2^- \rightarrow NO, D}} \cdot \frac{C_{DOC}}{C_{DOC} + K_{DOC, NO_2^- \rightarrow NO, D}} \cdot \frac{I_{O_2, NO_2^- \rightarrow NO}}{C_{O_{2,a}} + I_{O_2, NO_2^- \rightarrow NO}} \quad (6b)$$

$$r_{NO \rightarrow N_2O, D} = -\mu_{NO \rightarrow N_2O, D} \cdot X_{DEN} \cdot \frac{C_{NO,a}}{C_{NO,a} + K_{NO, NO \rightarrow N_2O, D}} \cdot \frac{C_{DOC}}{C_{DOC} + K_{DOC, NO \rightarrow N_2O, D}} \cdot \frac{I_{O_2, NO \rightarrow N_2O}}{C_{O_{2,a}} + I_{O_2, NO \rightarrow N_2O}} \quad (7b)$$

$$r_{N_2O \rightarrow N_2} = -\mu_{N_2O \rightarrow N_2} \cdot X_{DEN} \cdot \frac{C_{N_2O,a}}{C_{N_2O,a} + K_{N_2O, N_2O \rightarrow N_2}} \cdot \frac{C_{DOC}}{C_{DOC} + K_{DOC, N_2O \rightarrow N_2}} \cdot \frac{I_{O_2, N_2O \rightarrow N_2}}{C_{O_{2,a}} + I_{O_2, N_2O \rightarrow N_2}} \quad (8b)$$

where  $r_{A \rightarrow B}$  represents the production rate of  $B$  from  $A$ ,  $\mu_{A \rightarrow B}$  represents the maximum reaction rate of  $B$  from  $A$ ,  $K_{C, A \rightarrow B}$  represents the half-saturation concentration of  $C$  during the conversion from  $A$  to  $B$ ,  $I_{C, A \rightarrow B}$  represents the inhibition constant of  $C$  during the conversion from  $A$  to  $B$ ,  $X_{AOB}$ ,  $X_{NOB}$  and  $X_{DEN}$  represent the biomass content of ammonia-oxidizing bacteria, nitrite-oxidizing bacteria and denitrifiers, respectively.  $C_A$  represents the concentration of  $A$ . The subscripts of  $N$  and  $D$  refer to the individual process. The subscript of  $a$  represents aqueous gases, i.e., dissolved gases, to distinguish them from gaseous gases. More descriptions about the parameters can be found in the Supplementary information (SI) Table S1 and Table S2.

The contribution of nitrification and denitrification to  $N_2O$  production is assumed to depend on the  $NO_2^-$  content derived from nitrification and denitrification, that is, the N fluxes from  $NH_4^+$  and  $NO_3^-$  to  $NO_2^-$ . Since  $NO_3^-$  is simultaneously consumed by denitrification and replenished by nitrification

(Fig. 1b), the total N fluxes from initial  $NH_4^+$  to  $NO_2^-$  ( $F_N$ ) and from initial  $NO_3^-$  to  $NO_2^-$  ( $F_D$ ) can be calculated as

$$F_N = \int_0^{t_1} r_{NH_4^+ \rightarrow NO_2^-} dt \quad (9)$$

$$F_D = \int_0^{t_1} r_{NO_3^- \rightarrow NO_2^-} dt \cdot \frac{m_{NO_3,0}}{m_{NO_3,0} + \int_0^{t_1} r_{NO_2^- \rightarrow NO_3^-} dt} \cdot \frac{\int_0^{t_1} r_{NH_4^+ \rightarrow NO_2^-} dt}{\int_0^{t_1} (r_{NH_4^+ \rightarrow NO_2^-} + r_{NO_3^- \rightarrow NO_2^-}) dt} \quad (10)$$

where  $t_1$  is the reaction time, and  $m_{NO_3,0}$  is the initial amount of  $NO_3^-$ . The numerical calculation of  $F_N$  and  $F_D$  during the simulations can be found in the Supplementary information “Methods” section.

Therefore, the contribution ratio of denitrification ( $C_D$ ) to  $N_2O$  production can be calculated by

$$C_D = \frac{F_D}{F_N + F_D} \quad (11)$$

and the contribution ratio of nitrification to  $N_2O$  production equals  $1 - C_D$ .

### Process-based models quantifying $N_2O$ production and emissions

The developed process-based models accounted for the production and consumption of different N species, including  $NH_4^+$ ,  $NO_3^-$ ,  $NO_2^-$ , and  $N_2O$ , during the processes of nitrification and denitrification. The two models with and without transport were developed to examine the effect of transport on  $N_2O$  production and emissions from soils.

In the process-based model with transport (PBM-T-NF), the vertical transport is included. Since the soil water was stagnant during the simulation, the advection process related to water movement was neglected in our study. Only the diffusion of aqueous and gaseous species within soils was included in the developed models. The governing equations are described by

$$\frac{\partial C_i}{\partial t} = \frac{\partial}{\partial x} \left( D_i \frac{\partial C_i}{\partial x} \right) + r_i \quad (12)$$

where  $C_i$  is concentration of dissolved (i.e., aqueous, including  $\text{NH}_4^+$ ,  $\text{NO}_3^-$ ,  $\text{NO}_2$ , and DOC) or gaseous species (including  $\text{NH}_3$ ,  $\text{NO}$ ,  $\text{N}_2\text{O}$ ,  $\text{N}_2$ , and  $\text{O}_2$ ), and  $D_i$  is the effective diffusion coefficient. The values of  $D_i$  for aqueous ( $D_{i,a}$ ) and gaseous ( $D_{i,g}$ ) species can be calculated by following equations (Hamamoto et al. 2010)

$$\frac{D_{i,a}}{D_{i,a,0}} = \phi^{m_a - n_a} \theta^{n_d} \quad (13)$$

$$\frac{D_{i,g}}{D_{i,g,0}} = \phi^{m_g - n_g} (\phi - \theta)^{n_s} \quad (14)$$

where  $D_{i,a,0}$  and  $D_{i,g,0}$  are the corresponding diffusion coefficients in pure water and air,  $\phi$  is porosity,  $\theta$  is volumetric soil moisture,  $m_a$ ,  $n_a$  and  $m_g$ ,  $n_g$  are empirical parameters accounting for the effect of tortuosity and pore connectivity on diffusion of aqueous and gases species, respectively, in soils.

The term  $r_i$  is the sources or sinks of  $C_i$ , and was calculated according to the reaction pathways (Eqs. 1a–8a) and the corresponding reaction rates (Eqs. 1b–8b).  $r_i = 0$  for the gaseous species. The gaseous and aqueous gases, including  $\text{NH}_3$ ,  $\text{NO}$ ,  $\text{N}_2\text{O}$ ,  $\text{N}_2$ , and  $\text{O}_2$ , are assumed to reach equilibrium in each numerical voxel following the Henry's law (Sander 2015):

$$C_{i,a} = \frac{C_{i,g}}{K_{i,eqi}} \quad (15)$$

where  $C_{i,a}$  is the concentration of aqueous gas,  $C_{i,g}$  is the concentration of gaseous gas, and  $K_{i,eqi}$  is Henry's law constant.

In the process-based model without transport (PBM-NF), the mass transport was ignored and all physicochemical constituents were assumed to be uniformly distributed in the soil. The governing equations can be simplified into

$$\frac{\partial C_i}{\partial t} = r_i \quad (16)$$

The gas exchange rates between the soil and the headspace, including N gases emissions and  $\text{O}_2$  uptake, are calculated using Fick's law (Yan et al. 2018a):

$$R_i = D_{i,a} \frac{C_{i,a,top} - C_{i,headspace} K_{i,eq}}{\Delta x/2} + D_{i,g} \frac{C_{i,g,top} - C_{i,headspace}}{\Delta x/2} \quad (17)$$

where  $C_{i,a,top}$  and  $C_{i,g,top}$  are the concentrations of aqueous and gaseous gas in the top numerical voxel, respectively.  $C_{i,headspace}$  is the concentration of gas in the headspace,  $K_{i,eq}$  is the Henry constant, and  $\Delta x$  is the spatial resolution of numerical voxel.

The adsorbed and dissolved  $\text{NH}_4^+$  in each numerical voxel are assumed to be in equilibrium according to the Langmuir model [see Supplemental information equation (S1)]. The dissolved  $\text{NH}_4^+$  and dissolved  $\text{NH}_3$  are assumed to reach equilibrium in each numerical voxel as a function of pH [see Supplemental information equation (S2)]. The dissolved organic carbon (DOC) is assumed to be replenished by adsorbed organic carbon (SOC) via desorption [see Supplemental information equation (S3)].

#### Model calibration and validation

The process-based models with and without transport, in which  $\text{N}_2\text{O}$  sources are partitioned by tracking N flows, were calibrated and validated using laboratory incubation experiments.

The experiments measured  $\text{N}_2\text{O}$  production from nitrification and denitrification in two different fluvo-aquic soils by using the enriched  $^{15}\text{N}$  tracing technique (Wang et al. 2023). Soil samples (0–15 cm) were collected in October 2020 from two long-term agricultural experimental sites [Luan Cheng (LC), Hebei (37°53' N, 114°41'E) and Shang Zhuang (SZ), Beijing (39°48'N, 116°28'E)] in the North China Plain. The cropping system was rotated with winter wheat and summer maize in the LC and SZ. The physicochemical properties of the two soils are listed in Table 1.

Incubation experiments were conducted to quantify  $\text{N}_2\text{O}$  production from nitrification and denitrification under 40–100% water-filled pore space (WFPS).  $\text{K}^{15}\text{NO}_3$  (10.16 atom%) was applied at a rate of 50 mg  $\text{NH}_4^+\text{-N kg}^{-1}$  to identify the source of  $\text{N}_2\text{O-N}$ , and additional  $\text{NH}_4\text{Cl}$  was added at a rate of 50 mg  $\text{NO}_3^-\text{-N kg}^{-1}$ . Soil (20 g oven-dry equivalent) was added to each 120 mL incubation flask, with a bulk density of 1 g  $\text{cm}^{-3}$  and a soil depth of 8 mm. The flasks were pre-incubated in dark at 25 °C for 7 days, and then incubated for another 48 h after  $^{15}\text{N}$

**Table 1** Soil properties used for model calibration and validation

	Soil texture			pH	SOC (g kg <sup>-1</sup> )	NO <sub>3</sub> <sup>-</sup> -N (mg kg <sup>-1</sup> )	NH <sub>4</sub> <sup>+</sup> -N (mg kg <sup>-1</sup> )
	Sand (%)	Silt (%)	Clay (%)				
LC soil (model calibration)	29.2	64.1	6.7	7.92	19.82	30.49	2.08
SZ soil (model validation)	36.1	56.4	7.5	7.89	10.93	22.50	3.07

application. Concentrations and <sup>15</sup>N isotopic signatures of NH<sub>4</sub><sup>+</sup>, NO<sub>3</sub><sup>-</sup>, and N<sub>2</sub>O were measured after 12, 24, and 48 h. The concentrations of NH<sub>4</sub><sup>+</sup>-N and NO<sub>3</sub><sup>-</sup>-N were measured using a continuous-flow analyzer (Skalar Analytical, Breda, The Netherlands), and the concentrations of N<sub>2</sub>O were measured using gas chromatography (Agilent 7890, Santa Clara, CA, USA). Isotope analysis of NH<sub>4</sub><sup>+</sup>-N and NO<sub>3</sub><sup>-</sup>-N were performed on aliquots of the extracts using a diffusion technique (Brooks et al. 1989) and the <sup>15</sup>N isotopic signature was measured by isotope ratio mass spectrometry (IRMS 20–22, Sercon, Crewe, UK). The <sup>15</sup>N signature of N<sub>2</sub>O was determined using a Thermo Finnigan MAT-253 spectrometer (Thermo Fisher Scientific, Waltham, MA, USA).

The contribution ratios of nitrification,  $1 - C_D$ , and denitrification,  $C_D$ , to N<sub>2</sub>O production were calculated from the changes in <sup>15</sup>N atom% of NH<sub>4</sub><sup>+</sup>, NO<sub>3</sub><sup>-</sup>, and N<sub>2</sub>O by using the following equation (Stevens et al. 1997)

$$C_d = \frac{(a_{N_2O} - a_{NH_4})}{(a_{NO_3} - a_{NH_4})} \quad \text{with} \quad a_{NO_3} \neq a_{NH_4} \quad (18)$$

where  $a_{N_2O}$  is the <sup>15</sup>N atom% enrichment of the N<sub>2</sub>O produced by nitrification and denitrification, and  $a_{NO_3}$  and  $a_{NH_4}$  are the <sup>15</sup>N atom% enrichment of soil NO<sub>3</sub><sup>-</sup> and NH<sub>4</sub><sup>+</sup> at the time of gas sampling. More details about the experiments can be found in our previous experimental study (Wang et al. 2023).

The developed models were first calibrated with the experimental measurements of the LC soil and then validated with those of the SZ soil. The simulated concentrations of NH<sub>4</sub><sup>+</sup> and NO<sub>3</sub><sup>-</sup> as well as the N<sub>2</sub>O fluxes and  $C_D$  were compared with the measured values ( $n=48$ ). The simulated NH<sub>4</sub><sup>+</sup> and NO<sub>3</sub><sup>-</sup> concentrations as well as  $C_D$  were averaged over the soil profile in the PBM-T-NF model for comparisons with the measured ones. To minimize the effect of gas accumulation and transport inside soils on the PBM-NF model, the

experimental measurements over the first 12 h were used to calibrate and validate the developed models.

The eight maximum reaction rates ( $\mu_i$ , see Table S1) for nitrification and denitrification were first determined based on manual fitting. The values of  $\mu_i$  were then optimized using Markov Chain (MC) approach by randomly changing the parameter values 1000 times from half to twice the initial values (see Supplemental information “Results” section for parameterization) (Brooks 1998). The parameter values that produced the minimum accumulated normalized root mean square error ( $nRMSE$ ) of NH<sub>4</sub><sup>+</sup>, NO<sub>3</sub><sup>-</sup>, and N<sub>2</sub>O concentrations during the 10,000 times of simulations, were chosen, for which (Abdalla et al. 2020)

$$nRMSE = \frac{RMSE}{\bar{M}} \quad (19)$$

and

$$RMSE = \sqrt{\frac{\sum_{i=1}^n (S_i - M_i)^2}{n}} \quad (20)$$

where  $\bar{M}$  is the average of the measured values,  $S_i$  and  $M_i$  are the simulated and measured values under different moisture contents, and  $n$  is the treatment number of moisture contents (i.e.,  $n=6$ ).

#### Effects of model parameters and soil conditions

The influence of the maximum reaction rates ( $\mu_i$ ) on N<sub>2</sub>O emissions and sources ( $C_D$ ) under different soil moisture contents was evaluated by using the PBM-T-NF model. The experimental setup for model calibration was employed for the model sensitivity analysis (see Table 1). The effects of NH<sub>4</sub><sup>+</sup> and NO<sub>3</sub><sup>-</sup> concentrations, bulk density, and soil depth on N<sub>2</sub>O production and  $C_D$  were further investigated using the PBM-T-NF model. All parameters except the investigated factors remained unchanged during

the simulations (see Table 1, S1 and S2). The  $N_2O$  emissions and sources under different soil moisture contents were analyzed.

To further investigate the effect of vertical mass transport on  $N_2O$  emissions and sources, we created an artificial soil core with a height of 80 mm. The physicochemical properties in the artificial soil core were assigned the same as those of the experimental soil samples, and they were uniformly distributed along the soil depth. The dissolved and gaseous species could diffuse between adjacent layers, while the soil moisture was kept constant during the simulations. Unlike the closed system in other simulations, the soil core was assumed to be open to the atmosphere, mimicking the field situation, and its  $N_2O$  flux was calculated by Eq. (17), where the gas concentration in the headspace is the atmospheric concentration.

### Numerical setup and procedure

Matlab codes were developed to solve the governing equations. The simulated soils were considered as a single numerical voxel in the PBM-NF model and uniformly stratified in the PBM-T-NF model. The finite-difference method was used for the spatial discretization, and the spatial resolution of the numerical voxels ( $\Delta x$ ) was 1 mm. The explicit Euler method was used for the temporal evolution, and a small time step ( $\Delta t = 0.125$  s) was used to avoid negative values during the simulations. The initial concentrations of  $NH_4^+$  and  $NO_3^-$  used in the model evaluation simulation are presented in Supplemental information Table S3. The initial concentrations of SOC,  $O_2$ , and different N species and pH value were either obtained from literature or given by the experiments (see Supplemental information Table S1). The initial concentration of DOC was assumed to reach equilibrium with SOC, and the pH remained unchanged.

## Results

### Model calibration

Both the models with and without transport (PBM-T-NF and PBM-NF) overpredicted  $NH_4^+$  concentrations

at low soil moisture conditions (24.18% larger at  $WFPS=0.4$  and 20.05% larger at  $WFPS=0.6$ ), but underpredicted them at high soil moisture levels conditions except for  $WFPS=1.0$  (13.12% smaller at  $WFPS=0.8$  and 38.52% larger at  $WFPS=0.9$ , Fig. 2a). In contrast, the two models predicted  $NO_3^-$  concentrations well over the different soil moisture levels except for  $WFPS=1.0$  (averaged nRMSE is 13.58%, Fig. 2b). Compared to the PBM-NF model, the PBM-T-NF model produced much better  $N_2O$  concentrations across different soil moisture levels by capturing the low  $N_2O$  concentrations at low moisture levels (i.e.,  $WFPS=0.4$ ) and the high  $N_2O$  concentrations at high moisture levels (i.e.,  $WFPS=0.9$ ) (averaged nRMSE is 64.38% for PBM-NF and 36.35% for PBM-T-NF, Fig. 2c). The PBM-T-NF model also predicted the increasing trends of  $C_D$  with increasing soil moisture content (Fig. 2d), although it underestimated  $C_D$  under intermediate moisture conditions and overestimated it under low ( $WFPS=0.4$ ) and saturated ( $WFPS=1.0$ ) moisture conditions. In contrast, the PBM-NF model produced nearly constant  $C_D$  except for  $WFPS=1.0$ .

### Model validation

Both the PBM-T-NF and PBM-NF models captured the changing trends of  $NH_4^+$ ,  $NO_3^-$ , and  $N_2O$  concentrations with increasing soil moisture in the SZ soil. Compared with the PBM-NF model, the PBM-T-NF model produced more accurate  $NH_4^+$  (Fig. 3a) and  $NO_3^-$  (Fig. 3b) concentrations under high moisture conditions and much better  $N_2O$  concentration under relatively low soil moisture conditions (Fig. 3c). Furthermore, the PBM-T-NF model reliably reproduced the  $C_D$  as  $WFPS \geq 0.7$  (averaged nRMSE is 10.64%, Fig. 3d). By contrast, the PBM-NF model failed to capture the gradual increase in  $C_D$  as  $WFPS \geq 0.7$  (averaged nRMSE is 53.87%, Fig. 3d). Overall, the PBM-T-NF model well predicted the changes in all the four variables when soil moisture varied in a wide range, and it was used to evaluate the effects of model parameters and soil conditions on  $N_2O$  emissions and sources in the following sections.

### Sensitivity analysis

The maximum reaction rates,  $\mu_{NH_4^+-NO_2^-}$  and  $\mu_{NO_3^- - NO_2^-}$ , were found to significantly affect  $C_D$ .

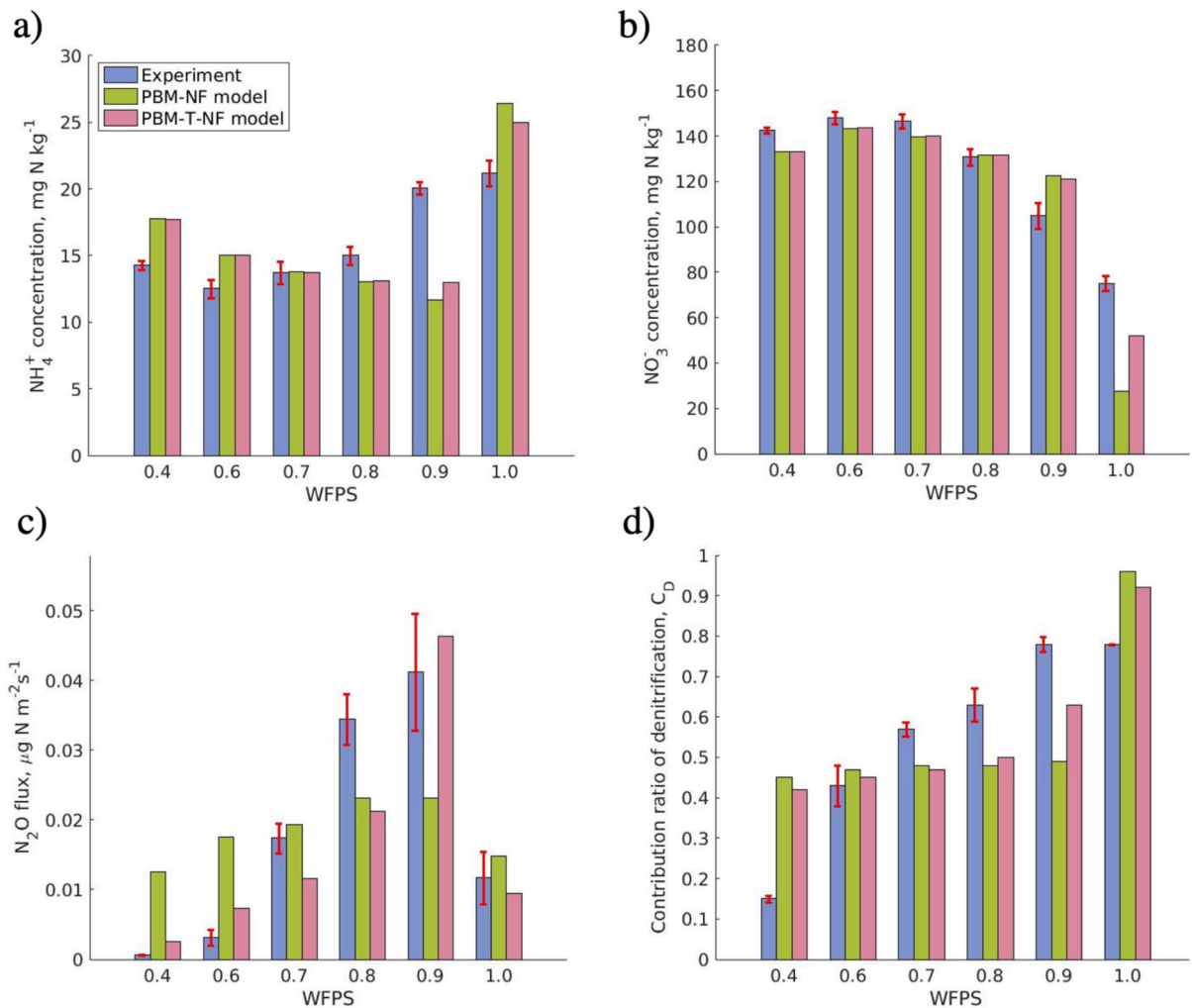


**Fig. 2** Comparisons of the measured and modelled **a** total  $\text{NH}_4^+$  concentration and **b** dissolved  $\text{NO}_3^-$  concentration at 12 h, and **c** soil  $\text{N}_2\text{O}$  fluxes and **d** contribution ratio of denitrifi-

cation to  $\text{N}_2\text{O}$  production,  $C_D$ , over the first 12 h. The experimental results of the LC soil were used to calibrate the developed models

Increased  $\mu_{\text{NH}_4^+ \rightarrow \text{NO}_2^-}$  reduced  $C_D$  especially under low soil moisture conditions (Fig. 4a). Conversely, increased  $\mu_{\text{NO}_3^- \rightarrow \text{NO}_2^-}$  promoted  $C_D$  across different moisture levels (Fig. 4b). By comparison, the effects of other maximum reactions rates, including  $\mu_{\text{NO}_2^- \rightarrow \text{NO}, \text{N}}$ ,  $\mu_{\text{NO} \rightarrow \text{N}_2\text{O}, \text{N}}$ ,  $\mu_{\text{NO}_2^- \rightarrow \text{NO}_3^-}$ ,  $\mu_{\text{NO}_2^- \rightarrow \text{NO}, \text{D}}$ ,  $\mu_{\text{NO} \rightarrow \text{N}_2\text{O}, \text{D}}$ ,  $\mu_{\text{N}_2\text{O} \rightarrow \text{N}_2}$ , can be neglected (results not show). However, all these parameters except  $\mu_{\text{NO} \rightarrow \text{N}_2\text{O}, \text{N}}$  modulated  $\text{N}_2\text{O}$  emissions (Fig. S1). Especially, increased  $\mu_{\text{NO}_2^- \rightarrow \text{NO}, \text{N}}$  (Fig. S1b) and  $\mu_{\text{NO}_3^- \rightarrow \text{NO}_2^-}$  (Fig. S1e) strongly promoted  $\text{N}_2\text{O}$  emissions, while increased  $\mu_{\text{NO}_2^- \rightarrow \text{NO}_3^-}$  (Fig. S1d) substantially depressed  $\text{N}_2\text{O}$  emissions.

### Effects of soil conditions on $\text{N}_2\text{O}$ sources and emissions

All four soil physiochemical properties clearly influenced  $C_D$ . Increased  $\text{NH}_4^+$  concentration significantly decreased  $C_D$  under relatively low moisture conditions, i.e.,  $\text{WFPS} \leq 0.8$  (Fig. 5a). In comparison, increased  $\text{NO}_3^-$  concentration slightly increased  $C_D$  over the different moisture conditions (Fig. 5b). Increased soil depth also promoted  $C_D$ , especially under high moisture conditions except for  $\text{WFPS} = 1.0$  (Fig. 5d). In contrast to the consistent effects of the above three soil properties across

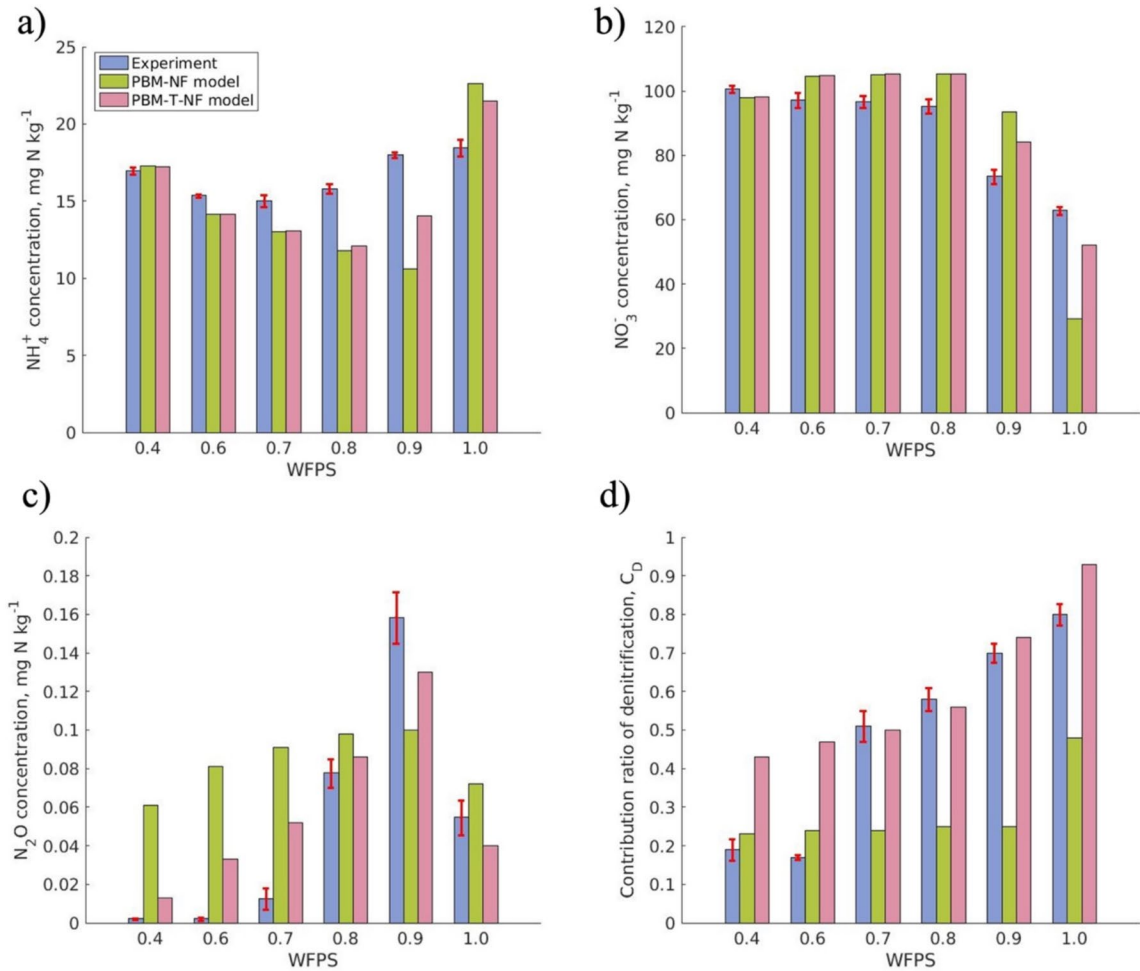


**Fig. 3** Comparisons of the measured and modelled **a** total  $\text{NH}_4^+$  concentration and **b** dissolved  $\text{NO}_3^-$  concentration at 12 h, and **c** soil  $\text{N}_2\text{O}$  flux and **d** contribution ratio of denitrifi-

cation to  $\text{N}_2\text{O}$  production,  $C_D$ , over the first 12 h. The experimental results of the SZ soil were used to validate the developed models

different moisture levels, increased bulk density reduced  $C_D$  at relatively low moisture levels but increased  $C_D$  under high moisture levels (Fig. 5c). Correspondingly, the increased  $\text{NH}_4^+$  concentration significantly increased  $\text{N}_2\text{O}$  emissions (Fig. S2a), while the other three soil properties have minor effects on  $\text{N}_2\text{O}$  emissions (Fig. S2b-d).

$\text{N}_2\text{O}$  emissions and sources from the artificial soil core under different moisture levels

The  $\text{N}_2\text{O}$  flux from the artificial soil core first increased and then decreased with increasing soil

moisture, reaching the maximum under  $\text{WFPS}=0.8$  (Fig. 6a). The  $\text{N}_2\text{O}$  flux approaches zero at  $\text{WFPS}=1.0$ , because the  $\text{N}_2\text{O}$  was almost completely denitrified to  $\text{N}_2$  under saturated conditions. Correspondingly,  $C_D$  increased with soil moisture, reaching almost 100% at  $\text{WFPS}=1.0$  (Fig. 6b). With time, the  $\text{N}_2\text{O}$  flux decreased and  $C_D$  increased. In particular,  $\text{N}_2\text{O}$  decreased by 113% at  $\text{WFPS}=0.7$  from 12 to 24 h, while  $C_D$  increased by no more than 13% at all the moisture levels.

Figure 7 shows the profile distributions of  $\text{NH}_4^+$ ,  $\text{NO}_3^-$ ,  $\text{N}_2\text{O}$  and  $\text{O}_2$  concentrations along the soil depth under different soil moisture conditions at 12

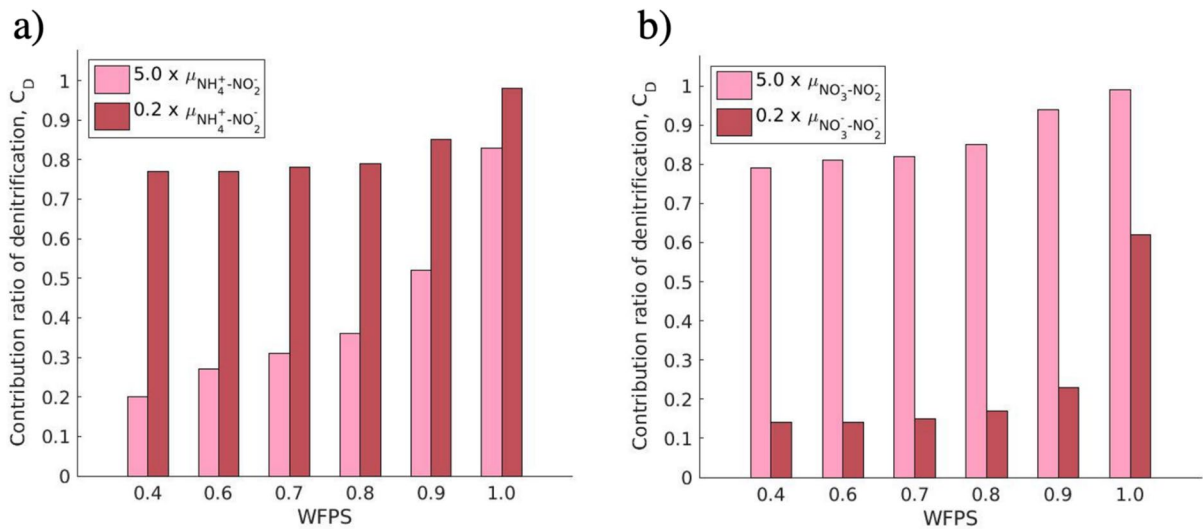


**Fig. 4** Simulated contribution ratio of denitrification to  $\text{N}_2\text{O}$  production,  $C_D$ , by the PBM-T-NF model as **a**  $\mu_{\text{NH}_4^+-\text{NO}_2^-}$  and **b**  $\mu_{\text{NO}_3^--\text{NO}_2^-}$  were increased (5.0  $\times$ ) or decreased (0.2  $\times$ ) by five

and 24 h. The  $\text{NH}_4^+$  was depleted rapidly throughout the soil profile under relatively low moisture conditions, and was mainly consumed in the top soil under high moisture conditions (Fig. 7a). Conversely,  $\text{NO}_3^-$  was mainly consumed at the bottom of the soil profile under high moisture conditions (Fig. 7b). Correspondingly,  $\text{N}_2\text{O}$  concentration is high under high moisture conditions (Fig. 7c), while  $\text{O}_2$  concentration is high under low moisture conditions (Fig. 7d).

## Discussion

### Performance of the developed models

The model with transport (PBM-T-NF) well predicted the concentrations of different N species under a wide range of soil moisture conditions. In particular, the PBM-T-NF model almost exactly predicted  $C_D$  under relatively high moisture conditions in the SZ soil, illustrating the robustness and accuracy of our proposed conceptual model based on N flows through the reaction pathways of nitrification and denitrification. By contrast, the model without transport (PBM-NF) could not capture the increasing trends in  $C_D$  with increasing soil moisture content, and failed to predict the rapid changes in  $\text{N}_2\text{O}$  concentrations around the

times. The LC soil was used to evaluate the effects of model parameters

maximum values, although the studied soil core is shallow (i.e., 8 mm). The results illustrate the necessity of considering mass transport in the simulation of soil N processes (Gilhespy et al. 2014; Tian et al. 2019). In particular, in contrast with the model neglecting diffusion, the model with transport predicted the  $\text{N}_2\text{O}$  emissions under high moisture contents much better, since the latter successfully captured the sharp decrease in  $\text{O}_2$  concentration along the soil profile, which favored denitrification and  $\text{N}_2\text{O}$  production (Rohe et al. 2021). The large  $\text{N}_2\text{O}$  fluxes have been widely demonstrated difficult to be predicted by models (Abdalla et al. 2020; Klier et al. 2011; Yue et al. 2019). Incorporating mass transport in these models may improve the prediction of  $\text{N}_2\text{O}$  emissions from soils.

The developed model assumed that  $\text{NO}_2^-$  derived from nitrification and denitrification was reduced indistinguishably to NO and then to  $\text{N}_2\text{O}$  by nitrifiers and denitrifiers. This explains why the simulated  $C_D$  was mainly sensitive to  $\mu_{\text{NH}_4^+-\text{NO}_2^-}$  and  $\mu_{\text{NO}_3^--\text{NO}_2^-}$ , whose values are crucial to control the contributing N flows from nitrification or denitrification. This assumption is appropriate in quasi-stationary conditions, where  $\text{N}_2\text{O}$  is produced by either nitrification or denitrification (Zhu et al. 2013), and is also the theoretical basis for the enriched isotopic approaches

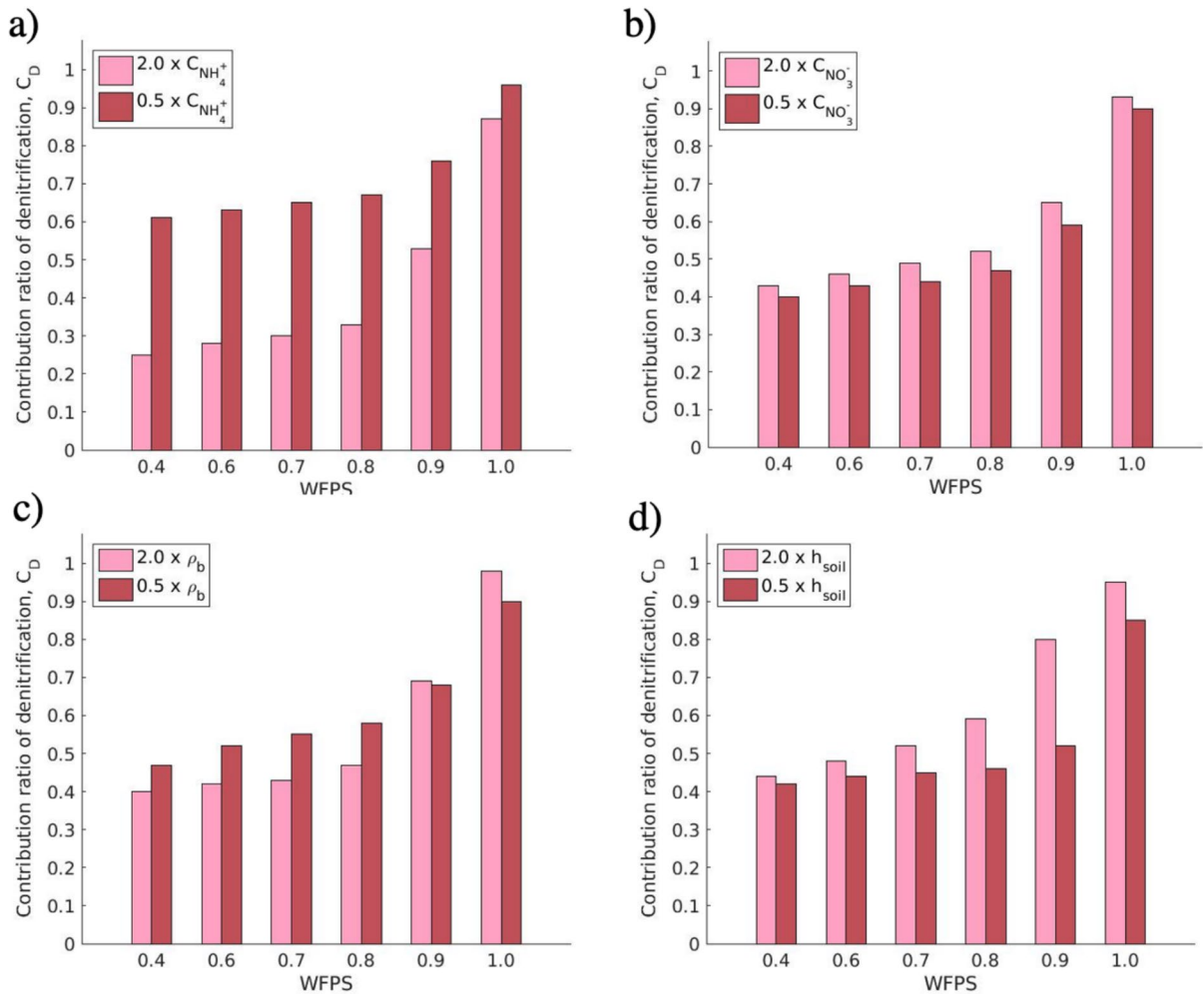


**Fig. 5** Simulated contribution ratio of denitrification to  $\text{N}_2\text{O}$  production,  $C_D$ , by the PBM-T-NF model as **a**  $\text{NH}_4^+$  concentration, **b**  $\text{NO}_3^-$  concentration, **c** bulk density, or **d** soil depth

(Bateman and Baggs 2005; Wang et al. 2023; Zhu et al. 2013). However, in dynamic environments such as riverine or coastal wetlands with fluctuating groundwater tables,  $\text{NO}_2^-$  produced by nitrification under aerobic conditions is often reduced by denitrification under anaerobic conditions (Deegan et al. 2012; Li et al. 2023). The coupled nitrification and denitrification process may be important for  $\text{N}_2\text{O}$  production in these land–water transition zones (Baggs 2011; Butterbach-Bahl et al. 2013), and complicates the modeling accuracy of our developed models.

was doubled ( $2.0 \times$ ) or halved ( $0.5 \times$ ). The LC soil was used to evaluate the effects of soil conditions

#### Effects of soil conditions on $\text{N}_2\text{O}$ sources and emissions

The PBM-T-NF model provides a feasible way to evaluate the effects of soil conditions on  $\text{N}_2\text{O}$  sources.  $\text{NH}_4^+$  concentration is found to be the key to regulating  $C_D$  in the soils studied (Fig. 5a), mainly because  $\text{NH}_4^+$  is the rate-limiting substrate for nitrification, whose product (i.e.,  $\text{NO}_3^-$ ) is substrate of denitrification (Li et al. 2024). If another soil with insufficient  $\text{NO}_3^-$  is used,  $\text{NO}_3^-$  may outperform  $\text{NH}_4^+$  in regulating  $C_D$  (Harris et al. 2021). Therefore, the baseline soil chemistry is critical to controlling the source of  $\text{N}_2\text{O}$ . In addition, elevated  $\text{NH}_4^+$  concentration not

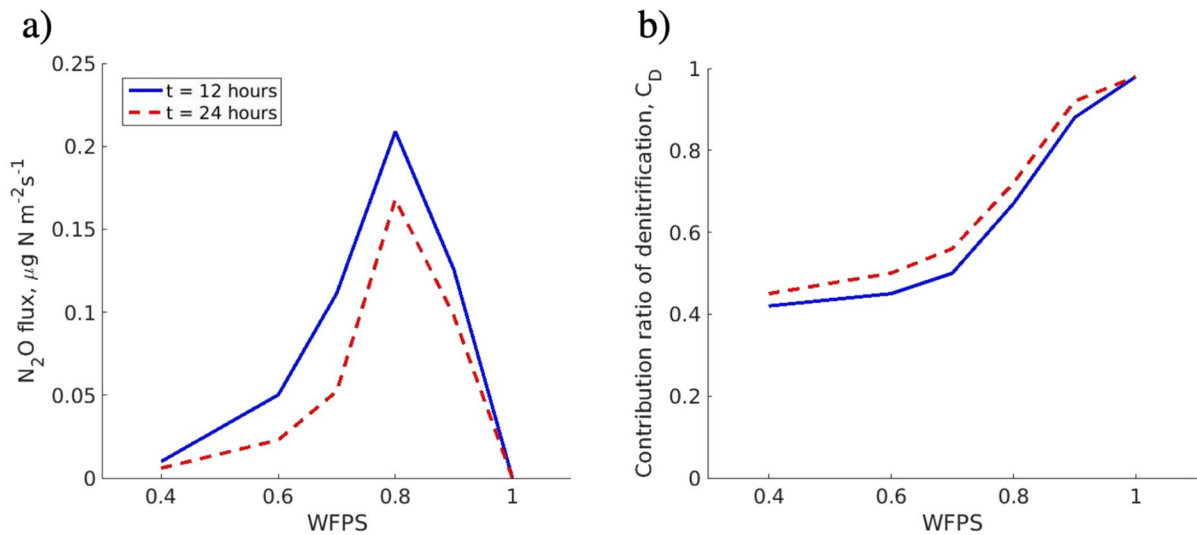


**Fig. 6** Simulated **a** N<sub>2</sub>O fluxes and **b** contribution of denitrification to N<sub>2</sub>O production,  $C_D$ , by the PBM-T-NF model in the artificial soil core under different soil moisture conditions at 12 and 24 h

only directly increases N<sub>2</sub>O production by promoting nitrification, but also indirectly stimulates it via denitrification by depleting O<sub>2</sub>, as NH<sub>4</sub><sup>+</sup> oxidation consumes O<sub>2</sub> and creates preferential conditions for denitrification (Song et al. 2019; Yang et al. 2021). This stimulation can become significant under high soil moisture conditions, where O<sub>2</sub> diffusion is limited (Smith 2017), and partially explains why the N<sub>2</sub>O flux increased by 6.8-folds at WFPS=0.9, though NH<sub>4</sub><sup>+</sup> concentration increased only by 4-folds (Fig. S2a).

It is plausible to assume that soil conditions regulating N<sub>2</sub>O production and its emission into the atmosphere interact. For example, elevated soil bulk density stimulated nitrification by increasing the rate-limiting NH<sub>4</sub><sup>+</sup> concentration under low moisture conditions, resulting in a smaller  $C_D$  (Fig. 5c). However, the elevated bulk density increased  $C_D$  under high moisture conditions by promoting denitrification, because it decreased O<sub>2</sub> diffusion into soils (Yan et al. 2016). The moisture-dependent effects of soil bulk density illustrate that the conclusions derived from controlled experiments under optimal moisture levels should be interpreted carefully in the field (Huang et al. 2015; Li et al. 2024). It is worth noting that the effect of soil compaction on N<sub>2</sub>O emission is currently attracting much attention (Ren et al. 2020). Similarly, increasing soil depth increased  $C_D$

by promoting denitrification, as it created a more anaerobic soil layer favorable for denitrification at the bottom of the soil core. The magnitude of the depth effect also depended on soil moisture content and was maximized at relatively high moisture contents (Fig. 5d), as O<sub>2</sub> was not limited at low soil moisture contents and N<sub>2</sub>O was reduced to N<sub>2</sub> under high moisture contents (Wang et al. 2020b). Therefore, multifactorial experiments with varying soil moisture are essential to unravel the underlying mechanisms behind the spatial and temporal changes in N<sub>2</sub>O fluxes and sources.

#### Effects of mass transport on N<sub>2</sub>O sources

The large differences between the simulation results from the PBM-T-NF model and the PBM-NF model underscore the importance of mass transport within soils, as do the simulated discrepancies from the shallow soil and the artificial soil core. For example, the simulated  $C_D$  from the soil core is apparently increased at WFPS=0.8 and 0.9 (Fig. 6b), compared to the results from the shallow soil. This is mainly because O<sub>2</sub> concentration was depleted at the bottom of the soil core, which strongly stimulated denitrification (Fig. 7 and Fig. S2). Compared with the shallow soil, the greater depth in the soil core also shifted the optimal moisture, under which the maximum N<sub>2</sub>O

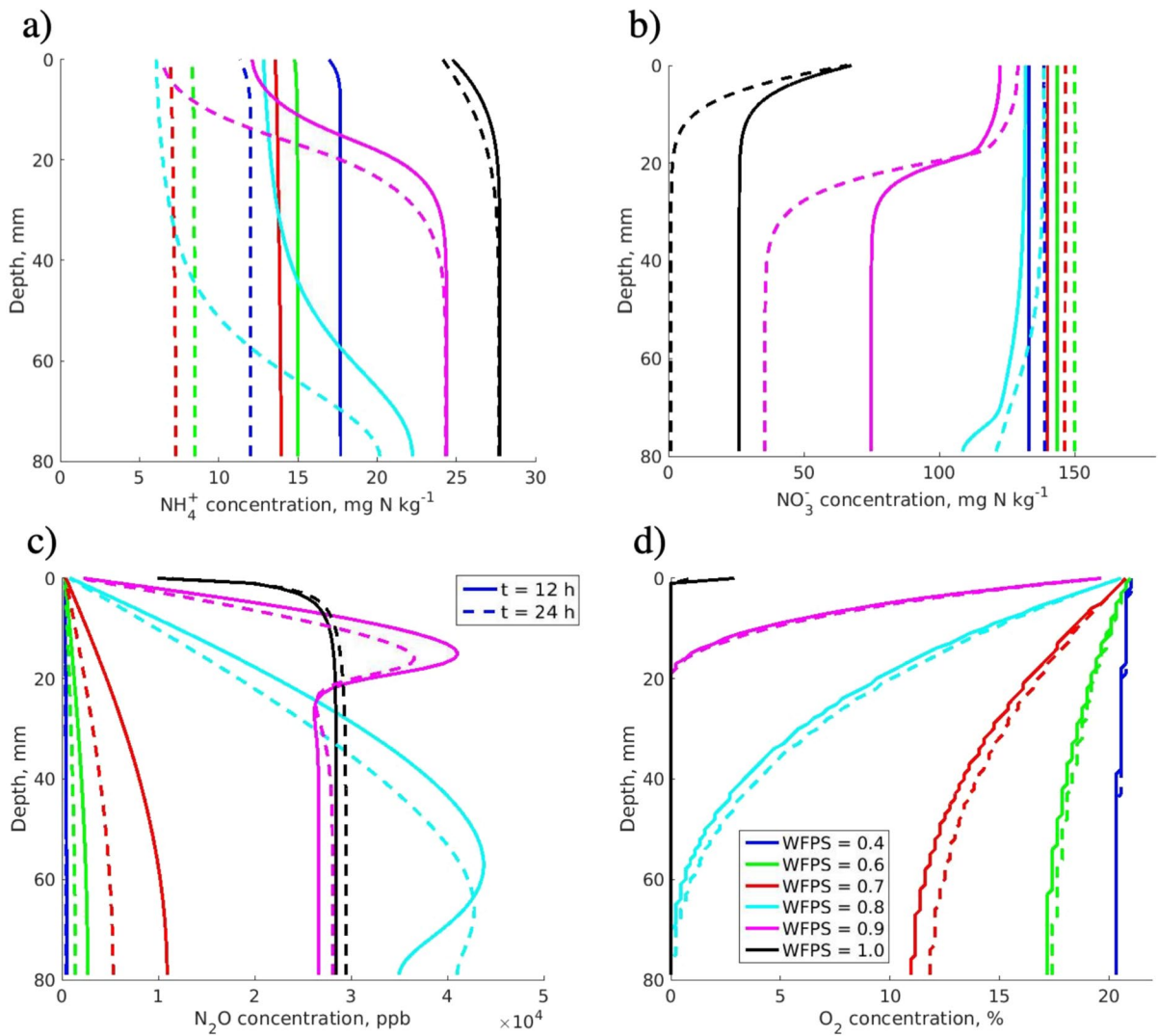


**Fig. 7** Simulated profile concentrations of **a** total  $\text{NH}_4^+$ , **b** dissolved  $\text{NO}_3^-$ , **c** gaseous  $\text{N}_2\text{O}$ , and **d** gaseous  $\text{O}_2$  by the PBM-T-NF model along the artificial soil core under different soil moisture conditions

flux occurred, from  $\text{WFPS}=0.9$  to  $0.8$ , as it further reduced  $\text{N}_2\text{O}$  to  $\text{N}_2$  via complete denitrification under the high moisture conditions (Fig. 7 and Fig. S2) (Hu et al. 2015; Xia et al. 2018). The anaerobic condition at the bottom of the soil core also explains why the  $\text{N}_2\text{O}$  flux approached zero at  $\text{WFPS}=1.0$  (Fig. 6a). The decline in gas diffusivity due to elevated soil moisture content has been found to well explain  $\text{N}_2\text{O}$  fluxes under different soil moisture conditions (Chamindu Deepagoda et al. 2019). The incorporation of gas diffusion in models have been found to improve the prediction of  $\text{N}_2\text{O}$  emissions especially under high

precipitation (Klier et al. 2011). Furthermore, soil water movement (i.e., advection) has been reported to affect N cycling and  $\text{N}_2\text{O}$  emissions by modulating substrate availability and moisture distribution (Gao et al. 2023), and its inclusion in process-based models could improve the simulation accuracy of N processes (Smith et al. 2020). Our model should also account for water movement in the future especially under high moisture conditions, where water is supposed to move downward due to gravity.

Soil  $\text{N}_2\text{O}$  emissions into the atmosphere are a function of  $\text{N}_2\text{O}$  production, transport and consumption

(Klier et al. 2011; Signor and Cerri 2013). A large number of studies have investigated  $N_2O$  production under different environmental conditions by using different types of soils (Bateman and Baggs 2005; Wang et al. 2023; Zhu et al. 2013). While  $N_2O$  production pathways are relatively better understood, the effects of transport on  $N_2O$  emissions are poorly understood, mainly because soil is an invisible and complex matrix containing solid, water, and gaseous phases (Rabot et al. 2018; Yan et al. 2023). Solute transport in soils regulates  $N_2O$  production through affecting substrate availability (Kravchenko et al. 2017), while gas transport in soils affects  $N_2O$  consumption by determining its residence time (Chang et al. 2022; Niu et al. 2016). Furthermore, the gas transport determines both  $N_2O$  production and consumption by controlling  $O_2$  availability (Van der Weerden et al. 2012). Therefore, mass transport is extremely important for soil  $N_2O$  emissions, and it is regulated by many factors including soil structure and moisture content (Kravchenko et al. 2017). Although the well-mixed soils (without structure) were employed to simulate  $N_2O$  emissions, the large difference between the simulation results from the developed models with and without transport indicate the importance of mass transport. This importance is expected to increase for  $N_2O$  emissions from natural soils, which contain structures such as different sizes of aggregates and complex pore connectivity (Van der Weerden et al. 2012; Fu et al. 2024).

#### Model limitations and future directions

The PBM-T-NF model provides a feasible way to quantify  $N_2O$  sources, overcoming the shortcomings of isotopic approaches, which are costly and subject to uncertainty (Denk et al. 2017). However, the model we developed focuses on nitrification and denitrification, which can lead to misleading results due to the incomplete N processes (Yan et al. 2024). For example, dissimilatory nitrate reduction to ammonium (DNRA) and anaerobic ammonium oxidation (ANAMMOX) may be important sources of  $N_2O$  under high moisture conditions (Shi et al. 2024), and their omission may lead to an overestimation of the  $N_2O$  contribution from nitrification or denitrification. Besides, abiotic processes including  $NH_2OH$  decomposition and chemodenitrification may contribute significantly to  $N_2O$  production (Zhu-Barker et al.

2015). Nitrogen mineralization and assimilation can also modulate  $N_2O$  production by regulating substrate and  $O_2$  availability (Xu et al. 2024; Yan et al. 2024; Zhang et al. 2022, 2018). Therefore, future models should incorporate these N processes in quantifying  $N_2O$  sources by tracking N flows in the corresponding reaction pathways, similar to what we did in this study. By combining with more sensitive experiments, including dual isotope approaches and site preference techniques (Kool et al. 2007; Wei et al. 2023), the advanced model can be calibrated and the comprehensive N processes are simulated more accurately.

Although the PBM-T-NF model was well validated on independent soils in this study, the model should be tested on more different types of soil in the future. For example, the contribution of denitrification to  $N_2O$  in acid soils may be significantly different from the alkaline soils as used in this study (Kool et al. 2011; Zhu et al. 2013), given that pH significantly impacts the community structures of nitrifiers and denitrifiers (Han et al. 2024). In addition, more experiments investigating the effects of soil and environmental conditions are needed to further constrain model parameters, and the dynamics of N processes should be experimentally quantified. Once our model is calibrated and validated by more experimental data using different soils and under various environmental conditions, it has the potential to be applied to a wide range of soil types and to capture the spatiotemporal variability of  $N_2O$  sources, which can guide us to take more precise measures to mitigate  $N_2O$  emissions from soils.

#### Conclusions

We developed process-based models to quantify  $N_2O$  attributions from nitrification and denitrification by tracking the N flows through the reaction pathways. Compared to the model without transport, the model accounting for solute and gas diffusions better predicted the  $N_2O$  fluxes and sources under a wide range of soil moisture levels in two different soils, highlighting the importance of including mass transport in predicting  $N_2O$  emissions. Therefore, combining  $N_2O$  production, transport, and consumption in process-based models is able to improve prediction of  $N_2O$  emissions. Furthermore, the effects of soil conditions on  $N_2O$  sources were found to depend on substrate

availability and moisture status. Multifactorial experiments and modeling are needed to unravel the mechanisms underlying the large spatial and temporal variabilities in soil-to-atmosphere N<sub>2</sub>O fluxes. Overall, we provide a feasible way to quantify N<sub>2</sub>O production from nitrification and denitrification, complementing current experimental approaches in the study of N processes.

**Acknowledgements** We would like to thank Dr. Christoph Müller from the Justus Liebig University Giessen, Institute of Plant Ecology, Germany, for constructive suggestions. This work was financially supported by the National Natural Science Foundation of China (42293262, 42077009), the National Key Research and development Program of China (2022YFF1301002), and Haihe Laboratory of Sustainable Chemical Transformations and Tianjin Municipal Science and Technology Bureau (No. 21ZYJDJC00090). K.B.B. received additional funding by the Pioneer Center for Research in Sustainable Agricultural Futures (Land-CRAFT), DNRF grant number P2, Aarhus University, Denmark. N.J.S. acknowledges the financial support from EU projects (SUS-SOIL, NPower and CSR).

**Author contributions** All co-authors contributed to the study. Z. Y. incubated the idea, wrote the numerical codes, run the simulations, and wrote the first draft. Z. C. helped to analyze the data, and all authors contributed to improve the manuscript.

**Funding** The authors have not disclosed any funding.

**Data availability** The data used in this study are publicly available in the Zenodo repository at <https://doi.org/10.5281/zenodo.15230929>.

## Declarations

**Conflict of interest** The authors declare no conflict of interest.

**Open Access** This article is licensed under a Creative Commons Attribution-NonCommercial-NoDerivatives 4.0 International License, which permits any non-commercial use, sharing, distribution and reproduction in any medium or format, as long as you give appropriate credit to the original author(s) and the source, provide a link to the Creative Commons licence, and indicate if you modified the licensed material. You do not have permission under this licence to share adapted material derived from this article or parts of it. The images or other third party material in this article are included in the article's Creative Commons licence, unless indicated otherwise in a credit line to the material. If material is not included in the article's Creative Commons licence and your intended use is not permitted by statutory regulation or exceeds the permitted use, you will need to obtain permission directly from the copyright holder. To view a copy of this licence, visit <http://creativecommons.org/licenses/by-nc-nd/4.0/>.

## References

- Abdalla M, Song X, Ju X, Topp CFE, Smith P (2020) Calibration and validation of the DNDC model to estimate nitrous oxide emissions and crop productivity for a summer maize-winter wheat double cropping system in Hebei, China. *Environ Pollut* 262:114199
- Baggs EM (2011) Soil microbial sources of nitrous oxide: recent advances in knowledge, emerging challenges and future direction. *Curr Opin Environ Sustain* 3(5):321–327
- Bateman EJ, Baggs EM (2005) Contributions of nitrification and denitrification to N<sub>2</sub>O emissions from soils at different water-filled pore space. *Biol Fertil Soils* 41(6):379–388
- Brooks S (1998) Markov chain Monte Carlo method and its application. *J R Stat Soc Ser D Stat* 47(1):69–100
- Brooks P, Stark JM, McInteer B, Preston T (1989) Diffusion method to prepare soil extracts for automated nitrogen-15 analysis. *Soil Sci Soc Am J* 53(6):1707–1711
- Butterbach-Bahl K, Baggs EM, Dannenmann M, Kiese R, Zechmeister-Boltenstern S (2013) Nitrous oxide emissions from soils: How well do we understand the processes and their controls? *Philos Trans R Soc B Biol Sci* 368(1621):20130122
- Chamindu Deepagoda TKK, Jayarathne JRRN, Clough TJ, Thomas S, Elberling B (2019) Soil-gas diffusivity and soil-moisture effects on NO emissions from intact pasture soils. *Soil Sci Soc Am J* 83(4):1032–1043
- Chang B, Yan Z, Ju X, Song X, Li Y, Li S, Fu P, Zhu-Barker X (2022) Quantifying biological processes producing nitrous oxide in soil using a mechanistic model. *Biogeochemistry* 159:1–14
- Davidson EA, Keller M, Erickson HE, Verchot LV, Veldkamp E (2000) Testing a conceptual model of soil emissions of nitrous and nitric oxides. *Bioscience* 50(8):667–680
- Deegan LA, Johnson DS, Warren RS, Peterson BJ, Fleeger JW, Fagherazzi S, Wollheim WM (2012) Coastal eutrophication as a driver of salt marsh loss. *Nature* 490(7420):388–392
- Del Grosso SJ, Parton WJ, Mosier AR, Ojima DS, Kulmala AE, Phongpan S (2000) General model for N<sub>2</sub>O and N<sub>2</sub> gas emissions from soils due to denitrification. *Glob Biogeochem Cycles* 14(4):1045–1060
- Del Grosso SJ, Smith W, Kraus D, Massad RS, Vogeler I, Fuchs K (2020) Approaches and concepts of modelling denitrification: increased process understanding using observational data can reduce uncertainties. *Curr Opin Environ Sustain* 47:37–45
- Denk TRA, Mohn J, Decock C, Lewicka-Szczebak D, Harris E, Butterbach-Bahl K, Kiese R, Wolf B (2017) The nitrogen cycle: a review of isotope effects and isotope modeling approaches. *Soil Biol Biochem* 105:121–137
- Ehrhardt F, Soussana J-F, Bellocchi G, Grace P, McAuliffe R, Recous S, Sándor R, Smith P, Snow V, de Antoni MM, Basso B, Bhatia A, Brillì L, Doltra J, Dorich CD, Doro L, Fitton N, Giacomini SJ, Grant B, Harrison MT, Jones SK, Kirschbaum MUF, Klumpp K, Laville P, Léonard J, Liebig M, Lieffering M, Martin R, Massad RS, Meier E, Merbold L, Moore AD, Myrgeiotis V, Newton P, Pattey E, Rolinski S, Sharp J, Smith WN, Wu L, Zhang Q (2018) Assessing uncertainties in crop and pasture ensemble

- model simulations of productivity and N<sub>2</sub>O emissions. *Glob Change Biol* 24(2):e603–e616
- Friedl J, Scheer C, De Rosa D, Müller C, Grace PR, Rowlings DW (2021) Sources of nitrous oxide from intensively managed pasture soils: the hole in the pipe. *Environ Res Lett* 16(6):065004
- Fu Z, Yan Z, Li S-I (2024) Effects of soil pore structure on gas diffusivity under different land uses: characterization and modelling. *Soil Tillage Res* 237:105988
- Gao Y, Tian Y, Zhan W, Li L, Sun H, Zhao T, Zhang H, Meng Y, Li Y, Liu T, Ding J (2023) Characterizing legacy nitrogen-induced time lags in riverine nitrogen reduction for the Songhuajiang River Basin: source analysis, spatio-seasonal patterns, and impacts on future water quality improvement. *Water Res* 242:120292
- Gilhespy SL, Anthony S, Cardenas L, Chadwick D, Del Prado A, Li C, Misselbrook T, Rees RM, Salas W, Sanz-Cobena A, Smith P, Tilston EL, Topp CFE, Vetter S, Yeluripati JB (2014) First 20 years of DNDC (DeNitrification DeComposition): model evolution. *Ecol Model* 292:51–62
- Groffman PM, Altabet MA, Böhlke H, Butterbach-Bahl K, David MB, Firestone MK, Giblin AE, Kana TM, Nielsen LP, Voytek MA (2006) Methods for measuring denitrification: diverse approaches to a difficult problem. *Ecol Appl* 16(6):2091–2122
- Hamamoto S, Moldrup P, Kawamoto K, Komatsu T (2010) Excluded-volume expansion of Archie's law for gas and solute diffusivities and electrical and thermal conductivities in variably saturated porous media. *Water Resour Res* 46(6):6514
- Han B, Yao Y, Liu B, Wang Y, Su X, Ma L, Liu D, Niu S, Chen X, Li Z (2024) Relative importance between nitrification and denitrification to N<sub>2</sub>O from a global perspective. *Global Change Biol* 30(1):e17082
- Hansen S (2002) Daisy, a flexible soil–plant–atmosphere system model. *Report Dept Agric* 615:1
- Harris E, Diaz-Pines E, Stoll E, Schloter M, Schulz S, Duffner C, Li K, Moore KL, Ingrisch J, Reinthaler D, Zechmeister-Boltenstern S, Glatzel S, Brüggemann N, Bahn M (2021) Denitrifying pathways dominate nitrous oxide emissions from managed grassland during drought and rewetting. *Sci Adv* 7(6):eabb7118
- Harris E, Yu L, Wang YP, Mohn J, Henne S, Bai E, Barthel M, Bauters M, Boeckx P, Dorich C, Farrell M, Krummel PB, Loh ZM, Reichstein M, Six J, Steinbacher M, Wells NS, Bahn M, Rayner P (2022) Warming and redistribution of nitrogen inputs drive an increase in terrestrial nitrous oxide emission factor. *Nat Commun* 13(1):4310
- Heinen M (2006) Simplified denitrification models: overview and properties. *Geoderma* 133(3):444–463
- Hu H, Chen D, He J (2015) Microbial regulation of terrestrial nitrous oxide formation: understanding the biological pathways for prediction of emission rates. *FEMS Microbiol Rev* 39(5):729–749
- Huang T, Gao B, Hu X, Lu X, Well R, Christie P, Bakken LR, Ju X (2015) Ammonia-oxidation as an engine to generate nitrous oxide in an intensively managed calcareous Fluvo-aquic soil. *Sci Rep* 4(1):03950
- IPCC (2021) *Climate change 2021*
- Jansen-Willems AB, Zawallich J, Müller C (2022) Advanced tool for analysing <sup>15</sup>N tracing data. *Soil Biol Biochem* 165:108532
- Klier C, Gayler S, Haberbosch C, Ruser R, Stenger R, Flessa H, Priesack E (2011) Modeling nitrous oxide emissions from potato-cropped soil. *Vadose Zone Journal* 10(1):184–194
- Kool DM, Wrage N, Oenema O, Dolfing J, Van Groenigen JW (2007) Oxygen exchange between (de)nitrification intermediates and H<sub>2</sub>O and its implications for source determination of NO<sub>3</sub><sup>-</sup> and N<sub>2</sub>O: a review. *Rapid Commun Mass Spectrom* 21(22):3569–3578
- Kool DM, Dolfing J, Wrage N, Van Groenigen JW (2011) Nitrifier denitrification as a distinct and significant source of nitrous oxide from soil. *Soil Biol Biochem* 43(1):174–178
- Kravchenko AN, Toosi ER, Guber AK, Ostrom NE, Yu J, Azeem K, Rivers ML, Robertson GP (2017) Hotspots of soil N<sub>2</sub>O emission enhanced through water absorption by plant residue. *Nat Geosci* 10:496–500
- Laville P, Lehuger S, Loubet B, Chaumartin F, Cellier P (2011) Effect of management, climate and soil conditions on N<sub>2</sub>O and NO emissions from an arable crop rotation using high temporal resolution measurements. *Agri For Meteorol* 151(2):228–240
- Li C, Aber J, Stange F, Butterbach-Bahl K, Papen H (2000) A process-oriented model of N<sub>2</sub>O and NO emissions from forest soils: 1. Model development. *J Geophys Res Atmos* 105(D4):4369–4384
- Li X, Gao D, Li Y, Zheng Y, Dong H, Liang X, Liu M, Hou L (2023) Increased nitrogen loading facilitates nitrous oxide production through fungal and chemodenitrification in estuarine and coastal sediments. *Environ Sci Technol* 57(6):2660–2671
- Li Y, Wang Z, Ju X, Wu D (2024) Disproportional oxidation rates of ammonia and nitrite deciphers the heterogeneity of fertilizer-induced N<sub>2</sub>O emissions in agricultural soils. *Soil Biol Biochem* 191:109325
- Lucas M, Gil J, Robertson GP, Ostrom NE, Kravchenko A (2023) Changes in soil pore structure generated by the root systems of maize, sorghum and switchgrass affect in situ N<sub>2</sub>O emissions and bacterial denitrification. *Biol Fertil Soils*. <https://doi.org/10.1007/s00374-023-01761-1>
- Maggi F, Gu C, Riley WJ, Hornberger GM, Venterea RT, Xu T, Spycher N, Steefel C, Miller NL, Oldenburg CM (2008) A mechanistic treatment of the dominant soil nitrogen cycling processes: model development, testing, and application. *J Geophys Res Biogeosci* 113(G2):G02016
- Müller C, Laughlin RJ, Spott O, Rütting T (2014) Quantification of N<sub>2</sub>O emission pathways via a <sup>15</sup>N tracing model. *Soil Biol Biochem* 72:44–54
- Niu S, Classen AT, Dukes JS, Kardol P, Liu L, Luo Y, Rustad L, Sun J, Tang J, Templer PH, Thomas RQ, Tian D, Vicca S, Wang Y-P, Xia J, Zaehle S (2016) Global patterns and substrate-based mechanisms of the terrestrial nitrogen cycle. *Ecol Lett* 19(6):697–709
- Parton WJ, Mosier AR, Ojima DS, Valentine DW, Schimel DS, Weier K, Kulmala AE (1996) Generalized model for N<sub>2</sub> and N<sub>2</sub>O production from nitrification and denitrification. *Global Biogeochem Cycles* 10(3):401–412
- Rabot E, Cousin I, Hénault C (2015) A modeling approach of the relationship between nitrous oxide fluxes from

- soils and the water-filled pore space. *Biogeochemistry* 122(2–3):395–408
- Rabot E, Wiesmeier M, Schlüter S, Vogel HJ (2018) Soil structure as an indicator of soil functions: a review. *Geoderma* 314:122–137
- Ren X, Zhu B, Bah H, Raza ST (2020) How tillage and fertilization influence soil N<sub>2</sub>O emissions after forestland conversion to cropland. *Sustainability* 12(19):7947
- Rohe L, Apelt B, Vogel H-J, Well R, Wu G-M, Schlüter S (2021) Denitrification in soil as a function of oxygen availability at the microscale. *Biogeosciences* 18(3):1185–1201
- Ruser R, Flessa H, Russow R, Schmidt G, Buegger F, Munch JC (2006) Emission of N<sub>2</sub>O, N<sub>2</sub> and CO<sub>2</sub> from soil fertilized with nitrate: effect of compaction, soil moisture and rewetting. *Soil Biol Biochem* 38(2):263–274
- Sander R (2015) Compilation of Henry's law constants (version 4.0) for water as solvent. *Atmos Chem Phys* 15(8):4399–4981
- Shi Z, She D, Pan Y, Abulaiti A, Huang Y, Liu R, Wang F, Xia Y, Shan J (2024) Ditch level-dependent N removal capacity of denitrification and anammox in the drainage system of the Ningxia Yellow River irrigation district. *Sci Total Environ* 916:170314
- Signor D, Cerri CEP (2013) Nitrous oxide emissions in agricultural soils: a review. *Pesquisa Agropecuária Tropical* 43(3):322–338
- Smith KA (2017) Changing views of nitrous oxide emissions from agricultural soil: key controlling processes and assessment at different spatial scales. *Eur J Soil Sci* 68(2):137–155
- Smith W, Grant B, Qi Z, He W, VanderZaag A, Drury CF, Helmers M (2020) Development of the DNDC model to improve soil hydrology and incorporate mechanistic tile drainage: a comparative analysis with RZWQM2. *Environ Model Softw* 123:104577
- Song X, Ju X, Topp CFE, Rees RM (2019) Oxygen regulates nitrous oxide production directly in agricultural soils. *Environ Sci Technol* 53(21):12539–12547
- Stevens RJ, Laughlin RJ, Burns LC, Arah JRM, Hood RC (1997) Measuring the contributions of nitrification and denitrification to the flux of nitrous oxide from soil. *Soil Biol Biochem* 29(2):139–151
- Stumm W, Morgan JJ (1996) *Aquatic chemistry: chemical equilibria and rates in natural waters*. Wiley, New York
- Tian H, Yang J, Lu C, Xu R, Canadell JG, Jackson RB, Arneith A, Chang J, Chen G, Ciais P (2018) The global N<sub>2</sub>O model intercomparison project. *Bull Am Meteorol Soc* 99(6):1231–1251
- Tian H, Yang J, Xu R, Lu C, Canadell JG, Davidson EA, Jackson RB, Arneith A, Chang J, Ciais P, Gerber S, Ito A, Joos F, Lienert S, Messina P, Olin S, Pan S, Peng C, Saikawa E, Thompson RL, Vuichard N, Winiwarter W, Zaehle S, Zhang B (2019) Global soil nitrous oxide emissions since the preindustrial era estimated by an ensemble of terrestrial biosphere models: magnitude, attribution, and uncertainty. *Global Change Biol* 25(2):640–659
- Tian H, Xu R, Canadell JG, Thompson RL, Winiwarter W, Suntharalingam P, Davidson EA, Ciais P, Jackson RB, Janssens-Maenhout G, Prather MJ, Regnier P, Pan N, Pan S, Peters GP, Shi H, Tubiello FN, Zaehle S, Zhou F, Arneith A, Battaglia G, Berthet S, Bopp L, Bouwman AF, Buitenhuis ET, Chang J, Chipperfield MP, Dangal SRS, Dlugokencky E, Elkins JW, Eyre BD, Fu B, Hall B, Ito A, Joos F, Krummel PB, Landolfi A, Laruelle GG, Lauerwald R, Li W, Lienert S, Maavara T, Macleod M, Millet DB, Olin S, Patra PK, Prinn RG, Raymond PA, Ruiz DJ, Van Der Werf GR, Vuichard N, Wang J, Weiss RF, Wells KC, Wilson C, Yang J, Yao Y (2020) A comprehensive quantification of global nitrous oxide sources and sinks. *Nature* 586(7828):248–256
- Van der Weerden TJ, Kelliher FM, de Klein CAM (2012) Influence of pore size distribution and soil water content on nitrous oxide emissions. *Soil Research* 50(2):125–135
- Vinten A, Castle K, Jrm A (1996) Field evaluation of models of denitrification linked to nitrate leaching for aggregated soil. *Eur J Soil Sci* 47(3):305–317
- Wang Q, Zhou F, Shang Z, Ciais P, Winiwarter W, Jackson RB, Tubiello FN, Janssens-Maenhout G, Tian H, Cui X, Canadell JG, Piao S, Tao S (2020a) Data-driven estimates of global nitrous oxide emissions from croplands. *Natl Sci Rev* 7(2):441–452
- Wang R, Pan Z, Zheng X, Ju X, Yao Z, Butterbach-Bahl K, Zhang C, Wei H, Huang B (2020b) Using field-measured soil N<sub>2</sub>O fluxes and laboratory scale parameterization of N<sub>2</sub>O/(N<sub>2</sub>O+N<sub>2</sub>) ratios to quantify field-scale soil N<sub>2</sub> emissions. *Soil Biol Biochem* 148:107904
- Wang C, Amon B, Schulz K, Mehdi B (2021) Factors that influence nitrous oxide emissions from agricultural soils as well as their representation in simulation models: a review. *Agronomy* 11(4):770
- Wang H, Yan Z, Ju X, Song X, Zhang J, Li S, Zhu-Barker X (2023) Quantifying nitrous oxide production rates from nitrification and denitrification under various moisture conditions in agricultural soils: laboratory study and literature synthesis. *Front Microbiol*. <https://doi.org/10.3389/fmicb.2022.1110151>
- Wang H, Yan Z, Chen Z, Song X, Zhang J, Li S-L, Müller C, Ju X, Zhu-Barker X (2024) Microbial ammonium immobilization promoted soil nitrogen retention under high moisture conditions in intensively managed fluvo-aquic soils. *Biol Fertil Soils*. <https://doi.org/10.1007/s00374-024-01831-y>
- Watts SH, Seitzinger SP (2000) Denitrification rates in organic and mineral soils from riparian sites: a comparison of N<sub>2</sub> flux and acetylene inhibition methods. *Soil Biol Biochem* 32(10):1383–1392
- Wei H, Song X, Liu Y, Wang R, Zheng X, Butterbach-Bahl K, Venterea RT, Wu D, Ju X (2023) In situ 15N–N<sub>2</sub>O site preference and O<sub>2</sub> concentration dynami. *Global Change Biol* 2023:1
- Xia L, Lam SK, Wolf B, Kiese R, Chen D, Butterbach-Bahl K (2018) Trade-offs between soil carbon sequestration and reactive nitrogen losses under straw return in global agroecosystems. *Global Change Biol* 24(12):5919–5932
- Xu P, Li G, Zheng Y, Fung JCH, Chen A, Zeng Z, Shen H, Hu M, Mao J, Zheng Y, Cui X, Guo Z, Chen Y, Feng L, He S, Zhang X, Lau AKH, Tao S, Houlton BZ (2024) Fertilizer management for global ammonia emission reduction. *Nature* 626(8000):792–798
- Yan Z, Liu C, Todd-Brown KE, Liu Y, Bond-Lamberty B, Bailey VL (2016) Pore-scale investigation on the response of

- heterotrophic respiration to moisture conditions in heterogeneous soils. *Biogeochemistry* 131(1):121–134
- Yan Z, Bond-Lamberty B, Todd-Brown KE, Bailey VL, Li S, Liu C, Liu C (2018a) A moisture function of soil heterotrophic respiration that incorporates microscale processes. *Nat Commun* 9(1):2562
- Yan Z, Wang T, Wang L, Yang X, Smith P, Hilpert M, Li S, Shang J, Bailey V, Liu C (2018b) Microscale water distribution and its effects on organic carbon decomposition in unsaturated soils. *Sci Total Environ* 644:1036–1043
- Yan Z, Wang Z, Fu Z, Zhang Y, Peng X, Zheng J (2023) Microscale heterogeneity controls macroscopic soil heterotrophic respiration by regulating resource availability and environmental stress. *Biogeochemistry*. <https://doi.org/10.1007/s10533-023-01044-9>
- Yan Z, Chang B, Song X, Wang G, Shan J, Yang L, Li S-I, Butterbach-Bahl K, Ju X (2024) A microbial-explicit model with comprehensive nitrogen processes to quantify gaseous nitrogen production from agricultural soils. *Soil Biol Biochem* 189:109284
- Yang Y, Zhang H, Shan Y, Wang J, Qian X, Meng T, Zhang J, Cai Z (2019) Response of denitrification in paddy soils with different nitrification rates to soil moisture and glucose addition. *Sci Total Environ* 651:2097–2104
- Yang L, Zhang X, Ju X, Wu D (2021) Oxygen-depletion by rapid ammonia oxidation regulates kinetics of  $N_2O$ , NO and  $N_2$  production in an ammonium fertilised agricultural soil. *Soil Biol Biochem* 163:108460
- Yue Q, Cheng K, Ogle S, Hillier J, Smith P, Abdalla M, Ledo A, Sun J, Pan G (2019) Evaluation of four modelling approaches to estimate nitrous oxide emissions in China's cropland. *Sci Total Environ* 652:1279–1289
- Zhang J, Müller C, Cai Z (2015) Heterotrophic nitrification of organic N and its contribution to nitrous oxide emissions in soils. *Soil Biol Biochem* 84:199–209
- Zhang Y, Ding H, Zheng X, Cai Z, Misselbrook T, Carswell A, Müller C, Zhang J (2018) Soil N transformation mechanisms can effectively conserve N in soil under saturated conditions compared to unsaturated conditions in subtropical China. *Biol Fertil Soils* 54(4):495–507
- Zhang B, Zhou M, Zhu B, Xiao Q, Zheng X, Zhang J, Müller C, Butterbach-Bahl K (2022) Soil clay minerals: an overlooked mediator of gross N transformations in Regosolic soils of subtropical montane landscapes. *Soil Biol Biochem* 168:108612
- Zheng J, Fujii K, Koba K, Wanek W, Müller C, Jansen-Willems AB, Nakajima Y, Wagai R, Canarini A (2023) Revisiting process-based simulations of soil nitrite dynamics: tighter cycling between nitrite and nitrate than considered previously. *Soil Biol Biochem* 178:108958
- Zhu X, Burger M, Doane TA, Horwath WR (2013) Ammonia oxidation pathways and nitrifier denitrification are significant sources of  $N_2O$  and NO under low oxygen availability. *Proc Natl Acad Sci* 110(16):6328–6333
- Zhu-Barker X, Cavazos AR, Ostrom NE, Horwath WR, Glass JB (2015) The importance of abiotic reactions for nitrous oxide production. *Biogeochemistry* 126(3):251–267

**Publisher's Note** Springer Nature remains neutral with regard to jurisdictional claims in published maps and institutional affiliations.